Published in final edited form as:

Adv Mater Interfaces. 2025 April 07; 12(7): . doi:10.1002/admi.202400713.

Conjugation Strategies for Low Solubility Proteins to Single-Walled Carbon Nanotubes as a Sensitive Fluorescent Assay to Protease Activity

Sepehr Hejazi[1], **Nabila Masud**[2], **Md. Hasibul Hasan Hasib**[2], **Cole Bertrand**[1], **Anwesha Sarkar**[2], **Nigel F Reuel**[1]

[1]Chemical and Biological Engineering – Iowa State University, 618 Bissell Rd, Ames, IA 50011

[2]Electrical and Computer Engineering – Iowa State University, 618 Bissell Rd, Ames, IA 50011

Abstract

Recently, single-walled carbon nanotube-based optical biosensors have been shown to detect hydrolase activity directly on target substrates such as proteins and peptides. This study presents a metastable protein conjugation approach to immobilize more hydrophobic proteins and enhance the sensitivity of protease detection. The method combines covalent conjugation of substrate proteins via carbodiimide chemistry (EDC/NHS) with non-covalent polymer wrapping of SWCNT, in this case, carboxymethyl cellulose. The formation of protein-SWCNT complexes as a result of multi-site conjugation between the proteins and carboxyl groups, enabled iterative pelleting, washing, and resuspension steps to be applied to the probes which allowed for removal of unbound proteins and residual materials, enhancing the sensor's sensitivity by approximately threefold, reaching an LOD of 6.4 ng/ml in a 5 minute reaction. This immobilization approach is applied to the ECM proteins such as gelatin and collagen and used to detect ECM degrading enzymes' activity. ECM degrading enzymes caused a fluorescent intensity decrease of the SWCNT probes, enabling quantification of enzyme concentration between the range 160 ng/ml to 100 μg/ml within 5 minutes of reaction. This hybrid approach provides a rapid and sensitive platform for detecting extracellular degrading enzymes with potential applications in cancer diagnosis and prognosis, wound healing, high-throughput screening for enzyme inhibitors and drug discovery.

Graphical Abstract

Corresponding author – reuel@iastate.edu.

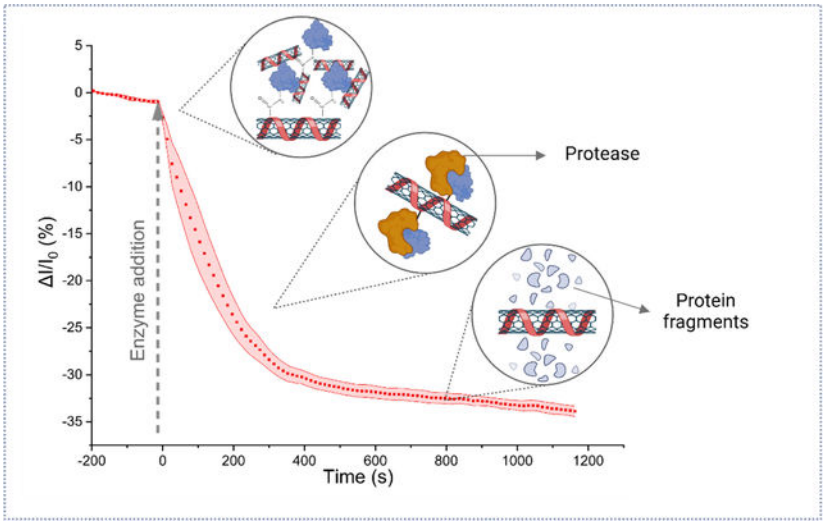

This study introduces a hybrid conjugation strategy for immobilizing low-solubility proteins on SWCNTs to enhance fluorescent detection of protease activity. By combining covalent conjugation with non-covalent polymer wrapping, the method achieves a threefold sensitivity increase, detecting protease activity in 5 minutes for ECM degrading enzymes and proteases.

Figure 1 a brief descreption of protein-SWCNT complex sensing mechanism

Keywords

SWCNT probes; ECM degrading enzymes; Collagen; Optical Biosensor

Introduction

Single-walled carbon nanotube (SWCNT) have been used for optical screening of biomolecules owing to many advantageous intrinsic properties such as photostability, chemical stability, high surface area, and near-infrared (NIR) fluorescence (870–2200 nm)[1]. They demonstrate the capability to sense a broad spectrum of biomolecules including proteins, nucleic acids, and metabolites. [2–4] SWCNTs have also recently been used in screening enzymatic activity and inhibition through various strategies involving the functionalization of the SWCNT surface with the substrate of interest[5]. This functionalization serves a dual purpose: it aids in dispersing inherently insoluble SWCNTs into an aqueous solution and also mediates a change in fluorescence signal upon substrate modification as solvent accessibility to the nanotube is affected.[5] These strategies can be categorized based on the type of binding between the substrate protein and the SWCNT surface into a) non-covalent, b) covalent, and c) hybrid approaches.[2,6]

Conventionally, covalent bonding strategies for functionalizing SWCNTs involve modifying their sidewalls through methods such as oxidation, which introduces carboxylic and hydroxyl groups on the nanotube surface that can be further conjugated.[7] While this approach can yield stable protein-SWCNT probes, it disrupts the sp^2-hybridized carbon lattice, often detrimental to the fluorescence of SWCNTs.[6] This disruption introduces

exciton trapping defects, leading to non-radiative recombination in some events.[8] It is important to note that recent advancements in engineered sparse defects have revealed enhancements of SWCNT spectral properties, such as quantum yield ; however the extent of modification needed for this work would be at a much higher surface coverage, eliminating these enhancing effects.[9,10]

Non-covalent binding depends on interactions between the hydrophobic regions of the substrate molecule and SWCNTs. In the case of protein substrates, π-stacking interactions of aromatic amino acids mediate association with the SWCNT[11]. Subsequently, the hydrophilic parts of the protein are leveraged to disperse the SWCNTs in the solution.[12] This strategy can be implemented by directly wrapping the SWCNT with substrate proteins or by wrapping the SWCNT with a surfactant molecule and performing a wrapping exchange with the substrate protein via dialysis.[13] Previously, our group demonstrated the capability of substrate-wrapped SWCNTs to monitor the activity of enzymes[14]. For instance, directly wrapped BSA-SWCNT was used to monitor the activity of bacterial protease.[15] However, this approach is dependent on the substrate protein's ability to achieve a stable dispersion of SWCNT[16], which poses challenges for other more insoluble proteins such as gelatin or collagen in forming stable biosensors.[17] Furthermore, the stability of these protein-SWCNT dispersions is influenced by factors such as pH and ionic strength of the solutions, rendering them unstable in many common buffers of interest.[18–20]

The hybrid approach combines elements of both previous strategies, employing a covalent conjugation of a protein to the non-covalently wrapped SWCNT. This enables more versatile protein immobilization, offering several advantages such as preserving the native form of the protein[6], facilitating the immobilization of proteins with low solubility onto SWCNTs, and enhancing the stability of SWCNTs through the use of an intermediate wrapping tailored to the biosensor application[21]. Previously, non-covalent wrappings such as poly(vinyl alcohol)[22], polyethylene glycol (PEG)derivatives[21], chitosan[23], pluronic P103[24], 1-Pyrenebutanoic Acid[25,26], and Triton X- have been utilized for this strategy. Carboxymethyl cellulose (CMC) has been employed to non-covalently wrap and disperse SWCNTs in solutions, offering high stability, non-toxicity, and biocompatibility.[27–29] Additionally, the abundance of active carboxyl group sites on carboxymethyl cellulose makes it a strong candidate for conjugation to protein substrates via carbodiimide (NHS/EDC) crosslinking, a method previously employed for protein immobilization.[30,31] However, in most studies to date, the excess unbound target substrate is left in solution, resulting in a competitive, non-reported target for enzyme degradation, thereby limiting the sensitivity of the assay. In this work, we devised methods to remove these unbound substrates using optimized carbodiimide cross-linking.

In this study, we employ a hybrid protein bonding approach and an iterative wash protocol to develop metastable solution-phase biosensors that can be temporarily precipitated to remove excess, unbound substrates from solution and thereby enhance the sensitivity of the enzyme screen. SWCNTs are initially dispersed with CMC to suspend them, and carbodiimide chemistry is used at an optimal ratio to form stable amide bonds between the CMC carboxyl groups and the surface lysins present in the target protein substrate. Enough proteins are bound to make a metastable solution that can be precipitated, washed, and resuspended.

Upon substrate degradation by an enzyme, the SWCNT fluorescence is attenuated. We apply this strategy to the development of functional probes for screening the activities of extracellular matrix (ECM) degrading enzymes against collagen and gelatin substrates.

ECMs regulate various cellular functions, including proliferation, adhesion, migration, differentiation, and death, especially relevant to tumor biology.[32] The constant remodeling and changes in the ECM are primarily governed by the interaction between adjacent cells and the ECM, mediated by the synthesis rate of ECM components and the secretion of enzymes for its degradation.[33] Metalloproteases are a large class of proteases accounting for 31% (148 known enzymes) of total human proteases[34]. Matrix metalloproteinases (MMPs) are a family of metalloproteases that were identified via their collagen degradation activity profile in 1962 [35]. With the completion of the Human Genome Project, 23 members of the MMP family were identified, emerging as primary enzymes accountable for degrading ECM components like collagen, gelatin, and elastin, while also regulating cytokine expression.[36] While commercial kits for screening the activity of ECM degrading enzymes such as MMPs exist, many of these are based on short sequence peptides that do not recapitulate the structural diversity of their target substrates. Therefore, we selected this to demonstrate SWCNT probes with enhanced sensitivity using complete collagen and gelatin target substrates.

Materials and method

SWCNT probes preparation

All chemicals were obtained from Sigma-Aldrich unless otherwise specified.

Preparation of CMC-SWCNT Suspension: Carboxymethyl cellulose (CMC, MW=700K, degree of substitution = 0.8) was dissolved in deionized (DI) water to a final volume of 3 ml, achieving a concentration of 2 mg/ml. Subsequently, CoMoCAT (6,5)-enriched single-walled carbon nanotubes (SWCNTs, CHASM SG65i, d = 0.78 nm) were added to a final concentration of 1 mg/ml. The mixture was sonicated using a Qsonica CL-18 tip sonicator at 6W power for 90 minutes in an ice bath. The resulting CMC-SWCNT suspension was centrifuged at 14,000 RCF for 30 minutes, and 80% of the supernatant was collected.

Activation of CMC-SWCNT: To adjust the pH to approximately 5, 10% (V/V) µl of 0.1 M MES buffer (pH = 4.5) was added to the SWCNT suspension. EDC (Thermo Scientific) and Sulfo-NHS (Thermo Scientific) were dissolved in DI water to concentrations ranging from 10 to 50 mg/ml, then added to the SWCNT solution to reach final concentrations of 4 mg/ml for EDC and 4.5 mg/ml for Sulfo-NHS, maintaining the same molar ratio. The mixture was vortexed for 30 seconds and then placed on an orbital shaker with 180 RPM at room temperature for 1 hour. To quench the EDC, 2-mercaptoethanol was added to a final concentration of 20 mM.

Protein Immobilization: The pH of the suspension was increased to 7.4 by adding 500 µl of 1 M NaOH. Next, PBS (1X, pH = 7.4) was added to reach 0.5 mg/ml of SWCNT in the solution .1mg/ml final concentration of Collagen type 1 (Gibco) form collagen-SWCNT, 1mg/ml final concentration of gelatin (Carolina) for gelatin SWCNT, 1mg/ml final

concentration of BSA for BSA-SWCNT, 0.5 mg/ml sfGFP which is synthesized and purified in our lab, 0.5 mg/ml final concentration of recombinant Protein A/G (Thermo Scientific), 0.5 mg/ml final concentration and Goat Anti-Human IgG Antibody IgG were then added to the SWCNT mixture and incubated at 4°C overnight to immobilize the proteins onto the CMC-SWCNT surface.

Washing and resuspension: Hydroxylamine was dissolved in 1X PBS to a final concentration of 10 mM, serving as a washing and storage buffer to quench the protein immobilization reaction by providing amine groups. After 16 hours, the SWCNT mixture was centrifuged at 12,000 RCF for 10 minutes to collect protein-CMC-SWCNT complexes at the bottom of the tube for the samples that produced aggregates (BSA, collagen, and gelatin). The supernatant was discarded, and 1 ml of washing buffer was added. The probes were resuspended via vortexing, and the washing process was repeated three times. Finally, 1–2 ml of washing buffer was added to the probes, which were then stored at 4°C. The resulting probes are easily resuspended in the solution using various methods, the least aggressive method is by pipetting, however for a better baseline stability, a 5-minute mild sonication using 0.5 W power (same sonication setup as SWCNT and CMC dispersion) is needed. For the samples without aggregation (IgG, Protein A/G, and sfGFP) the SWCNT solution was diluted 50 times in 1X PBS and tested.

SWCNT concentration measurements: All SWCNT concentration measurements were performed by measuring the absorbance at 661 nm of 100 µl of SWCNT solution in a 96-well plate. These measurements were compared to a SWCNT stock solution with a concentration of 1 mg/ml. To determine aggregation ratios, the absorbance of the SWCNT solution before adding protein was first measured (A_0) The SWCNT solutions were then centrifuged to form a pellet, and the absorbance of the unaggregated supernatant was measured (A_{sup}). The aggregation ratio (AR) was calculated using the following formula:

$$AR = 1 - \frac{A_{sup}}{A_0} \quad (1)$$

Enzymatic reaction and fluorescence measurement

SWCNT NIR fluorescence intensity signals were measured as detailed in our previous works using a custom NIR fluorimeter.[14,15] A brief schematic of the setup is presented in Supporting Figure S1. The temperature was maintained at 37°C using a custom heating module installed below the well plate holder. The SWCNT probes produced were diluted 100 to 300 times prior to the reaction (using the reader signal to reach a steady fluorescence between 6–9 mV) and then distributed in a 96-well plate.

Enzymes, including Collagenase from *Clostridium histolyticum* Type I, II, and IV, as well as recombinant human MMPs—MMP-1 (BioLegend), MMP-2 (AnaSpec), MMP-8 (BioLegend), and MMP-9 (BioLegend)—were prepared according to the manufacturers' recommended preparation and activation conditions. Heat inactivation of collagenases was achieved via incubating a 1mg/ml concentration of enzyme at 95°C for 30 minutes. Different

concentrations of the enzymes were added to the probes, and the signals were recorded. The relative signal change was calculated as below:

$$\frac{\Delta I}{Io} = \frac{I - I_0}{I_0 - I_{BG}} \quad (2)$$

Where I is the instantaneous signal, I_0 is the signal at time 0, and I_{BG} is the signal from an empty well. Additionally, signals were normalized with the control samples by subtracting the signal from the control.

AFM based high-resolution Imaging and characterization

AFM Sample preparation: Initially, atomic force microscopy (AFM)[37,38] compatible mica samples were prepared by gluing mica discs on top of stainless-steel metal specimen support discs (20 mm RS-MN-40-100020-50, Rave Scientific) and leaving those samples on the benchtop inside a 100×15 mm plastic dish to air dry overnight. Samples consisting of either SWCNT-protein or SWCNT without protein (each with a volume of 200 μl), were prepared. A circular muscovite mica disc (50–15, Highest Grade V1 AFM Mica Discs, 15 mm, Ted Pella), graded as V1, was freshly cleaved to ensure its surface was extremely flat, negatively charged, and ideal for coating the solution mentioned above for AFM measurements of SWCNT samples. The AFM experiments were performed on various types of samples, including fresh SWCNT (without protein), SWCNT with BSA at 100X dilution (both before and after degradation with 100 μg/ml of bacterial protease), SWCNT with collagen at 100X dilution (before and after degradation with100 μg/ml of collagenase type I), and SWCNT with gelatin at 100X dilution (before and after degradation with100 μg/ml of collagenase type I). Immediately after mica cleaving, the solution was dispersed carefully onto the mica substrate and incubated for 10 minutes at room temperature. Afterwards, the substrate was rinsed with deionized water (DI) and allowed to air dry inside the biosafety cabinet for 30 minutes before placing and securing the sample on the AFM stage through magnetic contact and conducting the AFM experiment.

AFM instrumentation and imaging parameters: BioScope Resolve system (Bruker) was used for the AFM imaging. A V-shaped SCANASYST-Air probe with a spring constant range of 0.3–0.8 N/m and a tip radius of 5 nm was used for scanning the SWCNT samples. AFM imaging was performed in Peakforce QNM in Air mode in a controlled vibration and noise isolation chamber to reduce the environmental noise in AFM data. Deflection sensitivity (30.358 nm/V) and cantilever spring constant (0.628 N/m) were calibrated each time after loading the sample on the AFM stage. AFM height sensor and peak force error images were taken at a steady scan rate of 0.303 Hz, with a peak force setpoint at 0.570 nN and peak force amplitude of 250 nm to prevent damage to the samples as well as the AFM probe and to ensure clear and detailed topographical characterization. Additionally, the imaging used a resolution of 256×256 pixels per line, and the peak force frequency was kept constant at 1 kHz during the entire characterization process.

AFM data analysis: Nanoscope Analysis and Gwyddion software were used to process and analyze the AFM images from the experiment, measuring the height of the SWCNTs with and without protein samples. This software helped extract structural details such as height, width, and topographical features of the samples from the images. For example, 67 nanotubes were selected from AFM images captured before protein degradation, and 56 nanotubes were selected from AFM images captured after degradation for image analysis of SWCNTs for BSA-SWCNT samples. For each tube, both the maximum height (representing the immobilized protein on the SWCNT) and the minimum height (serving as the background surface height) were examined. The difference between the maximum and minimum heights was defined as the protein height around SWCNT (Figure 3b). The averages were calculated for the height distributions, and a normal t-test was performed to measure the statistical significance.

Results and Discussion

1- Sensor design

The sensor design scheme involved sonication of SWCNTs with CMC to disperse them in solution, followed EDC/NHS mediated coupling to proteins at an optimal ratio for the probe metastability thereby enabling pelleting and washing of excess target substrate (Figure 1a,b). Achieving complete SWCNT surface coverage with CMC is crucial for stability, which can be optimized by adjusting the CMC to SWCNT ratio during sonication. Experimentation with different ratios revealed that a 2:1 mass ratio of CMC to SWCNT provides effective dispersion with minimal unsuspended SWCNTs (supporting information Figure S2). To minimize the exposure of bare SWCNT surfaces to the solution, we investigated the impact of CMC concentration by challenging the CMC-SWCNT probes with methylene blue (MB) dye, a known quencher that adsorbs onto exposed SWCNT surfaces that at lower CMC concentrations[39], there was a stronger quenching effect upon exposure to 1.2 μM MB, indicating insufficient coverage. In contrast, the 2:1 CMC to SWCNT ratio provided optimal coverage, as evidenced by minimal quenching (supporting information, Figure S3). Thus, we identified the 2:1 ratio as the most effective concentration for our study. The CMC's carboxyl groups were functionalized using EDC/NHS to form reactive NHS-esters; in the second step, the protein was added to complete the crosslinking. Initially, using EDC and NHS crosslinking agents led to SWCNT aggregation before protein addition, likely due to excessive modification of hydrophilic carboxyl groups on CMC. Substituting NHS with water-soluble sulfo-NHS improved probe's stability, and no aggregation was observed even at moderate EDC/NHS concentrations (see supporting Figure S4).

After protein immobilization, protein-CMC-SWCNT complexes are formed, facilitated by the presence of multiple activated carboxyl groups on CMC polymers and multiple amine sites on each protein. In some cases, such as with BSA, collagen, and gelatin, these complexes aggregated and could be pelleted down using centrifugal force, allowing the supernatant solution containing unbound protein substrates and residual chemicals from previous steps to be washed away (Figure 1b). We also assessed the same protocol with other proteins, such as sfGFP, Immunoglobulin G, and protein A. Interestingly, in these cases, we did not observe any notable aggregation of the protein-CMC-SWCNT complexes,

suggesting that the formation of protein-SWCNT aggregates likely depends on factors such as protein solubility and concentration. Thus, this approach is well-suited for more hydrophobic proteins.

2- Optimizing protein immobilization

First, we optimized the protein immobilization process by analyzing the impact of EDC/NHS amounts used for activating CMC on the efficiency of immobilization. Assuming that more aggregation after the immobilization step indicates higher success, BSA-CMC-SWCNT complexes were prepared with different EDC/NHS amounts. The immobilization efficiency after protein addition was calculated by measuring suspended SWCNT concentrations before and after protein addition (supporting Figure S5). At a 2:1 mass ratio of EDC and NHS to SWCNT, we observed the highest BSA-CMC-SWCNT aggregation ratio, and we proceeded with this amount for all further optimizations.

Next, we studied the effect of protein amounts used in the immobilization step by analyzing two factors: the aggregation ratio and the sensor's response to protease. First, we analyzed the formation of protein-CMC-SWCNT complexes by measuring the aggregated protein-SWCNTs after 24 hours of immobilization (Figure 2a). We observed different behaviors between BSA immobilization and collagen and gelatin. For BSA, higher aggregation was observed in samples with lower protein amounts. However, for collagen and gelatin samples, the aggregation ratio (AR) initially decreased with increasing protein concentration and then increased afterward. This suggests that at low concentrations, due to limited amine sites, more SWCNTs attach to a single protein, causing aggregation. For collagen and gelatin, which can polymerize and form higher molecular weight macromolecules (gels or fibers), using higher amounts leads to higher aggregation[40].

Next, we analyzed the dependency of the sensor enzyme response on the conjugated protein quantity used in the immobilization step by measuring the sensor's normalized fluorescence signal change five minutes after adding proteases. We observed a general trend for all the sensors tested: the performance improved with higher protein concentrations during the immobilization step, reaching a maximum (Figure 2b). This suggests that at higher protein concentrations, more proteins can attach to a single SWCNT, resulting in higher coverage of proteins around the tubes. This increased coverage likely leads to higher responses due to greater solvent access to the newly exposed surfaces of SWCNTs after protein degradation [15]. For gelatin and collagen probes, response to enzyme addition decreased at the highest ratio of protein to SWCNT (8:1). However, for BSA, performance remained at its highest level. This suggests that for gel-forming proteins, the large protein fibers that aggregate cause issues during the washing/resuspension step, as they cannot be effectively separated by washing and therefore are still present when used at high concentrations for sensor preparation, thereby reducing the sensor response.

3- Improving sensor sensitivity

As mentioned previously, aggregation is observed in some protein cases after the protein immobilization step, prompting a washing and resuspension step to enhance sensor performance by removing unbound proteins and residual chemicals. Collagen and gelatin

probes were prepared under the optimized conditions, and the performance of the sensors was evaluated with varying numbers of washing steps applied. The resulting sensors were exposed to discrete enzyme concentrations prepared in serial dilutions, and fluorescence signal changes were monitored over time. The limit of detection (LOD) and limit of quantification (LOQ) of the sensors were determined by selecting an enzyme concentration from the dilution series that corresponded to a signal greater than three times the standard deviation (3σ) of the control sample for the LOD, and greater than ten times the standard deviation (10σ) for the LOQ.[41] Sensors were fabricated by immobilizing both proteins and then tested with collagenase type 1 enzyme. Analysis of the signals after 5 minutes of enzyme reaction revealed that for both samples, the estimated LOQ improved with an increase in the number of washes applied to the probes, eventually reaching a final value of 160 ng/ml for both protein probes after 1 and 2 washes (Figure 2c). Additionally, the estimated LOD showed improvement after 3 washes, reaching 6.4 ng/ml (Figure 2d), indicating the importance of the washing step in improving sensor sensitivity (a two order of magnitude improvement over prior method with no excess substrate removal).

4- AFM to study probe mechanism

To confirm our proposed mechanism (Fig 1C) we first analyzed three different probe types, immobilized with BSA, gelatin, and collagen, using AFM. The AFM images provided detailed insights into the surface morphology of the probes and the aggregation of nanotubes and proteins. Protein-SWCNT complexes were observed in the AFM height and peak force error images, enhancing our understanding of their nanoscopic appearance. Initially, a more complex network of protein-SWCNT complexes was observed in all pre-degradation samples (Figure 3a). Proteins acted as joints, connecting SWCNTs and forming networked structures. In contrast, post-degradation samples exhibited more isolated SWCNTs with fewer proteins or lower protein coverage. Additionally, small protein fragments in the post-degradation samples indicated successful protein hydrolysis.

We analyzed the height of proteins on the SWCNT-covered areas before and after enzymatic degradation by measuring the peak height of protein-rich areas, which could be considered the diameter of the Protein-CMC-SWCNT tube (Figure 3b). Initially, we analyzed the CMC-SWCNT without any protein immobilization, finding the SWCNT heights ranged from 0.85 to 5 nm, with an average height of approximately 2.43 ± 1.09 nm (mean ± standard deviation). For BSA samples, the average height of proteins around the SWCNTs decreased from12.28 ± 4.32 nm to 6.67 ± 3.61 nm after enzymatic treatment, indicating protein size reduction around the SWCNTs (Figure 3c). Similarly, gelatin samples showed a height reduction from an average of 11.52 ± 4.39 nm to 8.83 ± 3.49 nm after enzymatic reaction. For collagen samples, the peak height decreased from 10.31 ± 3.61 nm to 5.20 ± 1.66 nm after enzymatic degradation.

Next, to determine whether the observed response of the nanotubes is due to hydrolysis or merely the enzyme's affinity to its substrate surrounding the SWCNTs, we conducted experiments with proteins known for their high binding affinities. Specifically, we tested two well-characterized interactions, IgG to protein A, and biotin to streptavidin.

First, Amine-PEG_2-biotin molecules were conjugated to the CMC-SWCNTs. Streptavidin, a protein with high affinity for biotin, was then added to the conjugated SWCNTs to evaluate the effect of streptavidin protein affinity on the sensor's response (Supporting Figure S7). The resulting affinity signals were opposite to that of our hydrolase response, observing fluorescence brightening. This increase was immediate and stable thereafter, with a 10% increase observed for 100 μg/ml streptavidin and a 5% increase for 20 μg/ml streptavidin. In a separate experiment, the affinity between IgG and Protein A/G was tested. First, IgG was immobilized on the SWCNTs, and Protein A/G was added as the target. This setup yielded a small 3% increase in signal at the highest target concentration, followed by a slow dissociation reducing the signal to 1.5%. Conversely, when Protein A/G was immobilized and IgG was added as the target, a similar signal was observed: the highest concentration of IgG increased the SWCNT fluorescence intensity by 4%, which then slowly decreased to 3%. In both cases, we attribute this brightening to a decrease in solvent access to the SWCNT surface upon protein binding. Therefore, the signal observed upon adding collagenases, which is a gradual reduction in fluorescence, suggests that this response is likely not due to the enzyme's affinity for its substrate. Instead, it indicates a degradation effect, as also supported by the AFM analysis.

5- Sensor response to ECM degrading enzymes

Next, we tested the probes against different commercial ECM degrading enzymes, specifically collagenase types I, II, and IV. The SWCNT fluorescence was monitored after adding different concentrations of collagenases, as well as heat-inactivated enzyme controls and buffer-only samples, to test the sensor's response to denatured proteins and the impact of the collagenase buffer. A reduction in fluorescent intensity is observed upon enzyme addition, which we attribute to increased solvent access caused by substrate degradation (Supporting Figures S6). The fast reaction time suggests that the enzymes start degrading single proteins immobilized on the nanotube's surface rather than degrading larger fibers or gels.[42] Approximately 10–30 minutes after the start of the reaction, higher concentrations of the enzymes reach a steady signal, while lower concentrations take more time to stabilize. Although signals can be read as end-point values, this approach has limitations, including nonspecific adsorption of hydrolyzed protein fragments, longer time requirements, and higher noise in the signal due to evaporation and SWCNT aggregation.

We found that the initial slope of the reaction can be calculated and correlated to the enzyme concentration used. The change in the normalized fluorescent signal after 5 minutes was plotted on a logarithmic scale with respect to enzyme concentrations, and the data fit a line well ($R^2 > 0.95$ in all cases) within the quantification range of each enzyme (Figure 4). To determine the lower and higher quantification range limits, different logarithmic trendline fittings were applied, and the widest enzyme concentration range that could be fit well (R^2 greater than 0.95) was selected. This fitting method has been previously employed in other commercial protease activity assays, such as the Pierce colorimetric assay [15].

For collagenase type I, both sensors performed similarly with a limit of detection (LOD) of 6.4 ng/ml and a lower limit of quantification (LOQ) of 160 ng/ml, aligning with the previous approach of analyzing signal strength in the washing step. For collagenase type II, the LOQ

in the collagen-immobilized sensor was 160 ng/ml, but in the gelatin-immobilized sensor, it was 800 ng/ml, and both achieved an LOD of 32 ng/ml. For collagenase type IV, the LOQ was 160 ng/ml for both proteins, but the LOD for the gelatin-immobilized sensor was 160 ng/ml, which is higher than the 32 ng/ml observed in the collagen-immobilized sensor.

As in other enzyme activity assays, the LOD can be improved by increasing incubation time with the probes. Therefore, we also tested the 24-hour responses to lower concentrations of collagenases to calculate the LOD of long reactions; we reached an LOD of 10 pg/ml to 1 ng/ml for all of the collagenases tested (see supporting Figures S8).

6- Selectivity of gelatin and collagen immobilized sensors to different MMPs.

This protein immobilization approach is a non-specific method that forms a covalent bond between lysine groups of the protein and the activated carboxyl groups on CMC wrappings. Therefore, no specific protein orientation is expected, raising the question if the immobilized proteins can act properly as a specific substrate for testing selective enzymes. We were interested in whether the responses of these two protein-nanotubes varied upon the addition of different MMPs, namely MMP-1, MMP-2, MMP-8, and MMP-9 enzymes. MMP-1 and MMP-8 are the most common MMPs that target fibrillar collagen substrates [43] while MMP-2 and MMP-9 are the most common enzymes that target gelatin substrates. [44] The normalized signal after 5 minutes of reaction with enzymes was recorded and a difference between the sensors' responses was observed (Figure 5). MMP-1 (500 ng/ml final concentration) and MMP-8 (500ng/ml final concentration) produced a greater signal in collagen-immobilized probes (5–10%), while MMP-2 (200 ng/ml final concentration) and MMP-9 (150 ng/ml final concentration) generated a stronger signal in gelatin-immobilized probes (1–10%), consistent with their selectivity for gelatin. It is important to note that MMP-2 and MMP-9 are reported to hydrolyze denatured collagens and lack activity on collagen fibrils. Therefore, assuming the sensor preparation method partially immobilized collagen in its denatured form, this response from MMP-2 and MMP-9 is expected.

Conclusion

In summary, the methods described here provide a versatile approach for manufacturing protein-SWCNT probes, suitable for applications such as enzyme activity screening and protein-protein interactions. In this study, ECM materials were effectively immobilized on SWCNTs using a hybrid conjugation technique that covalently bonds the protein to the non-covalent CMC wrapping of SWCNTs. This allows the actual substrate of ECM degrading enzymes to be immobilized with optical nanotubes, facilitating enzymatic reaction screening via the NIR fluorescence of SWCNTs. This method offers advantages over directly substrate-wrapped SWCNT biosensors, which are unstable in varying ionic strength and pH solutions due to the charge effects of protein-SWCNT interactions[45]. Also, the CMC wrapping acts as a surface pacifier which reduces the non-specific interactions with reaction components.

Another benefit of this method over traditional protease screening assays is its ability to measure the activity of proteases in interaction with their actual substrate. Unlike ELISA, which only measures protein concentrations, this method evaluates the protease

activity directly. An important finding was the role of protein-SWCNT aggregation post-immobilization, which aids in separating probes from unbound proteins and residual chemicals, significantly enhancing the LOD and LOQ of our biosensors. For instance, the LOD for gelatin-SWCNT decreased from 4 μg/ml to 6.4 ng/ml of collagenase Type I after three washing cycles. While nanotube-protein aggregation is generally viewed negatively for sensor quality, it can be beneficial depending on the biosensor application. This method allows for heightened sensitivity especially relevant for human health applications where implicated proteins may be present in very low quantities [46].

The rapid response following enzymatic degradation provides a more reliable readout compared to extended reaction signals, enabling protein quantification within five minutes. Fast response analysis is a more reliable readout since post-degradation interactions between SWCNTs and reaction products, which can re-adsorb to the nanotube, creates signal noise for long term reaction signals. Surface passivation strategies, such as pre-incubation with protein fragments, may help mitigate long-reaction noise, though this is beyond the scope of this work.

Future directions include developing more site-specific protein-SWCNT crosslinking strategies to preserve the accessibility of immobilized proteins to analytes, particularly through protein terminal reactions conjugation. This could improve the response of protein-protein interactions, facilitating the development of affinity assays such as antibody-antigen interactions.

Supplementary Material

Refer to Web version on PubMed Central for supplementary material.

References

(1). O'Connell MJ; Bachilo SM; Huffman CB; Moore VC; Strano MS; Haroz EH; Rialon KL; Boul PJ; Noon WH; Kittrell C; Ma J; Hauge RH; Weisman RB; Smalley RE Band Gap Fluorescence from Individual Single-Walled Carbon Nanotubes. Science 2002, 297 (5581), 593–596. 10.1126/science.1072631. [PubMed: 12142535]

(2). Ackermann J; Metternich JT; Herbertz S; Kruss S Biosensing with Fluorescent Carbon Nanotubes. Angew Chem Int Ed 2022, 61 (18), e202112372. 10.1002/anie.202112372.

(3). Kruss S; Hilmer AJ; Zhang J; Reuel NF; Mu B; Strano MS Carbon Nanotubes as Optical Biomedical Sensors. Advanced Drug Delivery Reviews 2013, 65 (15), 1933–1950. 10.1016/j.addr.2013.07.015. [PubMed: 23906934]

(4). Ferrier DC; Honeychurch KC Carbon Nanotube (CNT)-Based Biosensors. Biosensors 2021, 11 (12), 486. 10.3390/bios11120486. [PubMed: 34940243]

(5). Basu S; Hendler-Neumark A; Bisker G Monitoring Enzyme Activity Using Near-Infrared Fluorescent Single-Walled Carbon Nanotubes. ACS Sens 2024, acssensors.4c00377. 10.1021/acssensors.4c00377.

(6). Antonucci A; Kupis-Rozmysłowicz J; Boghossian AA Noncovalent Protein and Peptide Functionalization of Single-Walled Carbon Nanotubes for Biodelivery and Optical Sensing Applications. ACS Appl. Mater. Interfaces 2017, 9 (13), 11321–11331. 10.1021/acsami.7b00810. [PubMed: 28299937]

(7). Battigelli A; Ménard-Moyon C; Da Ros T; Prato M; Bianco A Endowing Carbon Nanotubes with Biological and Biomedical Properties by Chemical Modifications. Advanced Drug Delivery Reviews 2013, 65 (15), 1899–1920. 10.1016/j.addr.2013.07.006. [PubMed: 23856410]

(8). Chio L; Pinals RL; Murali A; Goh NS; Landry MP Covalent Surface Modification Effects on Single-Walled Carbon Nanotubes for Targeted Sensing and Optical Imaging. Adv Funct Materials 2020, 30 (17), 1910556. 10.1002/adfm.201910556.

(9). Kim M; McCann JJ; Fortner J; Randall E; Chen C; Chen Y; Yaari Z; Wang Y; Koder RL; Heller DA Quantum Defect Sensitization via Phase-Changing Supercharged Antibody Fragments. J. Am. Chem. Soc 2024, 146 (18), 12454–12462. 10.1021/jacs.4c00149. [PubMed: 38687180]

(10). Zaumseil J Luminescent Defects in Single-Walled Carbon Nanotubes for Applications. Advanced Optical Materials 2022, 10 (2), 2101576. 10.1002/adom.202101576.

(11). Wang C; Li S; Zhang R; Lin Z Adsorption and Properties of Aromatic Amino Acids on Single-Walled Carbon Nanotubes. Nanoscale 2012, 4 (4), 1146–1153. 10.1039/C1NR11073J. [PubMed: 22095051]

(12). Ouassil N; Pinals RL; Del Bonis-O'Donnell JT; Wang JW; Landry MP Supervised Learning Model Predicts Protein Adsorption to Carbon Nanotubes. Sci. Adv 2022, 8 (1), eabm0898. 10.1126/sciadv.abm0898. [PubMed: 34995109]

(13). Barone PW; Baik S; Heller DA; Strano MS Near-Infrared Optical Sensors Based on Single-Walled Carbon Nanotubes. Nature Mater 2005, 4 (1), 86–92. 10.1038/nmat1276. [PubMed: 15592477]

(14). Kuo M-T; Raffaelle JF; Waller EM; Varaljay VA; Wagner D; Kelley-Loughnane N; Reuel NF Screening Enzymatic Degradation of Polyester Polyurethane with Fluorescent Single-Walled Carbon Nanotube and Polymer Nanoparticle Conjugates. ACS Nano 2023, 17 (17), 17021–17030. 10.1021/acsnano.3c04347. [PubMed: 37606935]

(15). Kallmyer NE; Musielewicz J; Sutter J; Reuel NF Substrate-Wrapped, Single-Walled Carbon Nanotube Probes for Hydrolytic Enzyme Characterization. Anal. Chem 2018, 90 (8), 5209–5216. 10.1021/acs.analchem.7b05444. [PubMed: 29554802]

(16). Nepal D; Geckeler KE Proteins and Carbon Nanotubes: Close Encounter in Water. Small 2007, 3 (7), 1259–1265. 10.1002/smll.200600511. [PubMed: 17492743]

(17). Gillen AJ; Boghossian AA Non-Covalent Methods of Engineering Optical Sensors Based on Single-Walled Carbon Nanotubes. Front. Chem 2019, 7, 612. 10.3389/fchem.2019.00612. [PubMed: 31616652]

(18). Horn DW; Tracy K; Easley CJ; Davis VA Lysozyme Dispersed Single-Walled Carbon Nanotubes: Interaction and Activity. J. Phys. Chem. C 2012, 116 (18), 10341–10348. 10.1021/jp300242a.

(19). Pinals RL; Yang D; Rosenberg DJ; Chaudhary T; Crothers AR; Iavarone AT; Hammel M; Landry MP Quantitative Protein Corona Composition and Dynamics on Carbon Nanotubes in Biological Environments. Angew Chem Int Ed 2020, 59 (52), 23668–23677. 10.1002/anie.202008175.

(20). Holt BD; McCorry MC; Boyer PD; Dahl KN; Islam MF Not All Protein-Mediated Single-Wall Carbon Nanotube Dispersions Are Equally Bioactive. Nanoscale 2012, 4 (23), 7425. 10.1039/c2nr31928d. [PubMed: 23086474]

(21). Yeniyurt Y; Kilic S; Güner-Yılmaz ÖZ; Bozoglu S; Meran M; Baysak E; Kurkcuoglu O; Hizal G; Karatepe N; Batirel S; Güner FS Fmoc-PEG Coated Single-Wall Carbon Nanotube Carriers by Non-Covalent Functionalization: An Experimental and Molecular Dynamics Study. Front. Bioeng. Biotechnol 2021, 9, 648366. 10.3389/fbioe.2021.648366. [PubMed: 34055757]

(22). Yoon H; Ahn J; Barone PW; Yum K; Sharma R; Boghossian AA; Han J; Strano MS Periplasmic Binding Proteins as Optical Modulators of Single-Walled Carbon Nanotube Fluorescence: Amplifying a Nanoscale Actuator. Angew Chem Int Ed 2011, 50 (8), 1828–1831. 10.1002/anie.201006167.

(23). Reuel NF; Dupont A; Thouvenin O; Lamb DC; Strano MS Three-Dimensional Tracking of Carbon Nanotubes within Living Cells. ACS Nano 2012, 6 (6), 5420–5428. 10.1021/nn301298e. [PubMed: 22624495]

(24). Chen RJ; Bangsaruntip S; Drouvalakis KA; Wong Shi Kam N; Shim M; Li Y; Kim W; Utz PJ; Dai H Noncovalent Functionalization of Carbon Nanotubes for Highly Specific Electronic Biosensors. Proc. Natl. Acad. Sci. U.S.A 2003, 100 (9), 4984–4989. 10.1073/pnas.0837064100. [PubMed: 12697899]

(25). Chen RJ; Zhang Y; Wang D; Dai H Noncovalent Sidewall Functionalization of Single-Walled Carbon Nanotubes for Protein Immobilization. J. Am. Chem. Soc 2001, 123 (16), 3838–3839. 10.1021/ja010172b. [PubMed: 11457124]

(26). Besteman K; Lee J-O; Wiertz FGM; Heering HA; Dekker C Enzyme-Coated Carbon Nanotubes as Single-Molecule Biosensors. Nano Lett 2003, 3 (6), 727–730. 10.1021/nl034139u.

(27). Long L; Li F; Shu M; Zhang C; Weng Y Fabrication and Application of Carboxymethyl Cellulose-Carbon Nanotube Aerogels. Materials 2019, 12 (11), 1867. 10.3390/ma12111867. [PubMed: 31181867]

(28). Loghin F; Rivadeneyra A; Becherer M; Lugli P; Bobinger M A Facile and Efficient Protocol for Preparing Residual-Free Single-Walled Carbon Nanotube Films for Stable Sensing Applications. Nanomaterials 2019, 9 (3), 471. 10.3390/nano9030471. [PubMed: 30901851]

(29). Lu S; Bai L; Wen Y; Li M; Yan D; Zhang R; Chen K Water-Dispersed Carboxymethyl Cellulose-Montmorillonite-Single Walled Carbon Nanotube Composite with Enhanced Sensing Performance for Simultaneous Voltammetric Determination of Two Trace Phytohormones. J Solid State Electrochem 2015, 19 (7), 2023–2037. 10.1007/s10008-014-2695-5.

(30). Immobilization of Laccase from Trametes Hirsuta onto CMC Coated Magnetic Nanoparticles. IJE 2020, 33 (4). 10.5829/ije.2020.33.04a.01.

(31). Yang C-H; Chen C-A; Chen C-F Surface-Modified Cellulose Paper and Its Application in Infectious Disease Diagnosis. Sensors and Actuators B: Chemical 2018, 265, 506–513. 10.1016/j.snb.2018.03.092.

(32). Lu P; Takai K; Weaver VM; Werb Z Extracellular Matrix Degradation and Remodeling in Development and Disease. Cold Spring Harbor Perspectives in Biology 2011, 3 (12), a005058–a005058. 10.1101/cshperspect.a005058. [PubMed: 21917992]

(33). Bonnans C; Chou J; Werb Z Remodelling the Extracellular Matrix in Development and Disease. Nat Rev Mol Cell Biol 2014, 15 (12), 786–801. 10.1038/nrm3904. [PubMed: 25415508]

(34). De Almeida LGN; Thode H; Eslambolchi Y; Chopra S; Young D; Gill S; Devel L; Dufour A Matrix Metalloproteinases: From Molecular Mechanisms to Physiology, Pathophysiology, and Pharmacology. Pharmacol Rev 2022, 74 (3), 714–770. 10.1124/pharmrev.121.000349.

(35). Woessner J Catabolism of Collagen and Non-Collagen Protein in the Rat Uterus during Post-Partum Involution. Biochemical Journal 1962, 83 (2), 304–314. 10.1042/bj0830304. [PubMed: 14007838]

(36). McMahon M; Ye S; Pedrina J; Dlugolenski D; Stambas J Extracellular Matrix Enzymes and Immune Cell Biology. Front. Mol. Biosci 2021, 8, 703868. 10.3389/fmolb.2021.703868. [PubMed: 34527702]

(37). Masud N; Tang J; Hasib HH; Jubery T. (Zaki); Lee XX; Guo H; Sarkar A Correlating Macroscopic Plant Growth Parameters to Nanomechanical Properties of Cellulose Microfibrils. Current Plant Biology 2024, 38, 100345. 10.1016/j.cpb.2024.100345.

(38). Sarkar A Biosensing, Characterization of Biosensors, and Improved Drug Delivery Approaches Using Atomic Force Microscopy: A Review. Front. Nanotechnol 2022, 3, 798928. 10.3389/fnano.2021.798928.

(39). Zheng Y; Alizadehmojarad AA; Bachilo SM; Kolomeisky AB; Weisman RB Dye Quenching of Carbon Nanotube Fluorescence Reveals Structure-Selective Coating Coverage. ACS Nano 2020, 14 (9), 12148–12158. 10.1021/acsnano.0c05720. [PubMed: 32845604]

(40). Normand V; Muller S; Ravey J-C; Parker A Gelation Kinetics of Gelatin: A Master Curve and Network Modeling. Macromolecules 2000, 33 (3), 1063–1071. 10.1021/ma9909455.

(41). Lavín Á; Vicente J; Holgado M; Laguna M; Casquel R; Santamaría B; Maigler M; Hernández A; Ramírez Y On the Determination of Uncertainty and Limit of Detection in Label-Free Biosensors. Sensors 2018, 18 (7), 2038. 10.3390/s18072038. [PubMed: 29949904]

(42). Saini K; Cho S; Dooling LJ; Discher DE Tension in Fibrils Suppresses Their Enzymatic Degradation – A Molecular Mechanism for 'Use It or Lose It.' Matrix Biology 2020, 85–86, 34–46. 10.1016/j.matbio.2019.06.001.

(43). Loffek S; Schilling O; Franzke C-W Biological Role of Matrix Metalloproteinases: A Critical Balance. European Respiratory Journal 2011, 38 (1), 191–208. 10.1183/09031936.00146510. [PubMed: 21177845]

(44). Jabłońska-Trypuć A; Matejczyk M; Rosochacki S Matrix Metalloproteinases (MMPs), the Main Extracellular Matrix (ECM) Enzymes in Collagen Degradation, as a Target for Anticancer Drugs. Journal of Enzyme Inhibition and Medicinal Chemistry 2016, 31 (sup1), 177–183. 10.3109/14756366.2016.1161620. [PubMed: 27028474]

(45). Shumeiko V; Paltiel Y; Bisker G; Hayouka Z; Shoseyov O A Paper-Based Near-Infrared Optical Biosensor for Quantitative Detection of Protease Activity Using Peptide-Encapsulated SWCNTs. Sensors 2020, 20 (18), 5247. 10.3390/s20185247. [PubMed: 32937986]

(46). Granström LM; Ekman GE; Malmström A; Ulmsten U; Woessner JF Serum Collagenase Levels in Relation to the State of the Human Cervix during Pregnancy and Labor. American Journal of Obstetrics and Gynecology 1992, 167 (5), 1284–1288. 10.1016/S0002-9378(11)91701-3. [PubMed: 1442977]

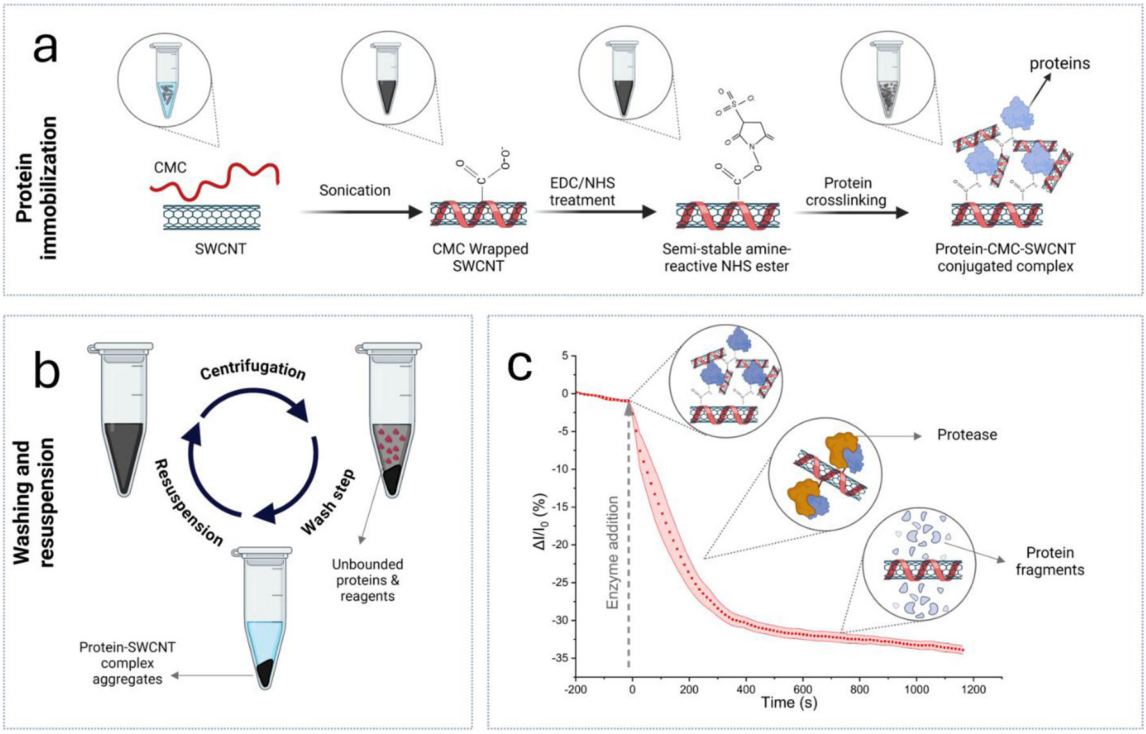

Figure 1:

a) Bioconjugation steps: SWCNTs and CMC are sonicated to create a CMC-wrapped SWCNT suspension. Carboxyl groups on the CMC were treated with EDC/NHS to form a semi-stable amine-reactive NHS ester. The substrate protein was then added, crosslinking the NHS ester with lysine amine groups, resulting in a protein-CMC-SWCNT conjugate that can form aggregates via multiple grafting on the same proteins. b) Washing Step: After protein immobilization, the conjugate forms a pellet at the tube bottom after moderate centrifugation, allowing for the removal of the supernatant containing unbound protein and excess NHS/EDC reagents. This process can be repeated by washing with buffer and resuspending using vortexing or pipetting, resulting in a final, cleaned sample free of background substrate. c) Example fluorescence response and hypothesized mechanism for protease activity detection. The initial fluorescence signal of SWCNTs is stable and quenches upon addition of enzyme due to degradation of substrate and increased solvent access. “Created in BioRender. Hejazi, S. (2025) https://BioRender.com/n03×368 “.

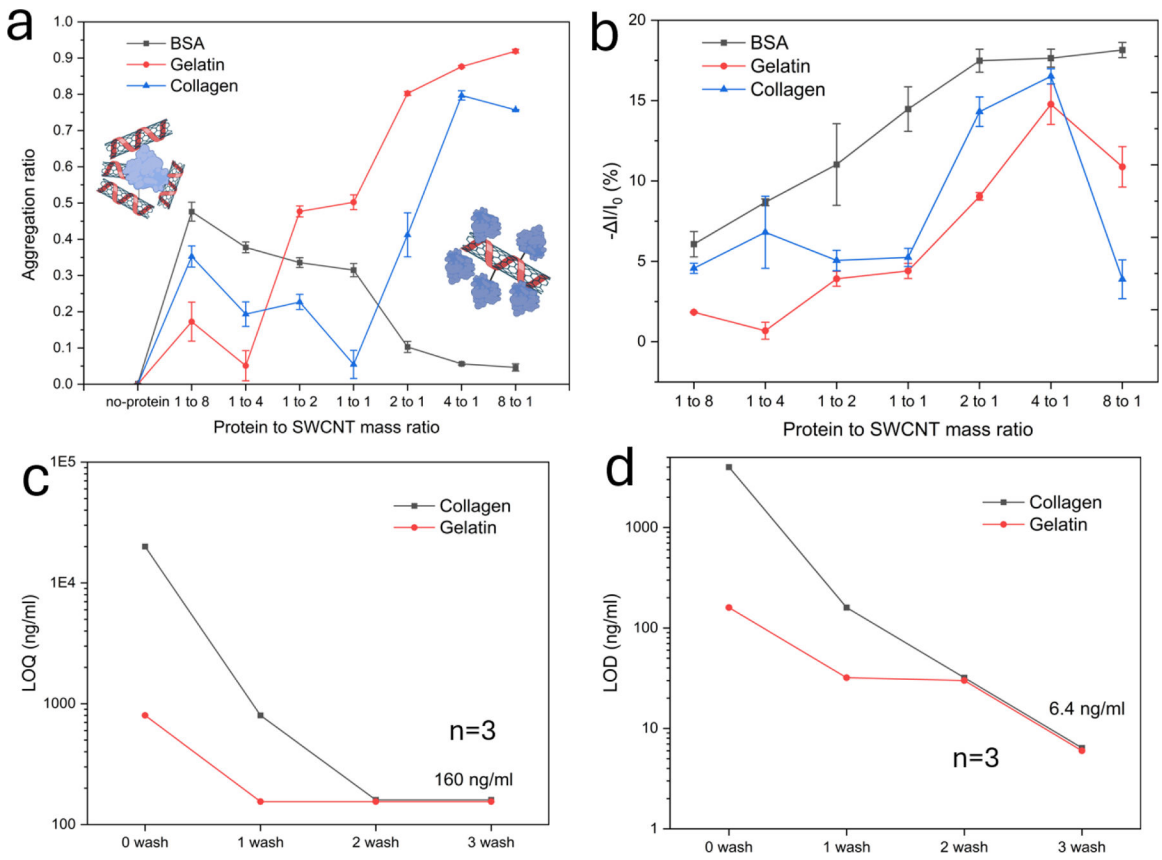

Figure 2.

Probe optimization: a) Impact of Protein Amounts on Aggregation Formation. The aggregation ratio was measured by comparing the absorbance level of unaggregated SWCNTs in the solution after protein immobilization compared to the SWCNT absorbance before adding the protein. Three different proteins capable of forming aggregates were tested in relation to varying protein amounts. b) Normalized Fluorescence Signal Change: The normalized fluorescence signal change of probes made with different protein amounts during the immobilization step was measured 5 minutes after adding 2 μg/ml of collagenase type I for collagen and gelatin immobilized samples, and 1μg/ml of bacterial protease for BSA immobilized samples. c,d) Effect of Washing Steps on LOQ and LOD: The impact of the number of washing steps on the LOQ and LOD of the sensors was examined. Replicates (n=3) of sensors were washed, resuspended, and serially diluted collagenase type I was added to gelatin and collagen immobilized samples. The control samples standard deviation was calculated, and the lowest enzyme concentration producing signals greater than 10 and 3 times the standard deviation were selected as LOQ and LOD, respectively.

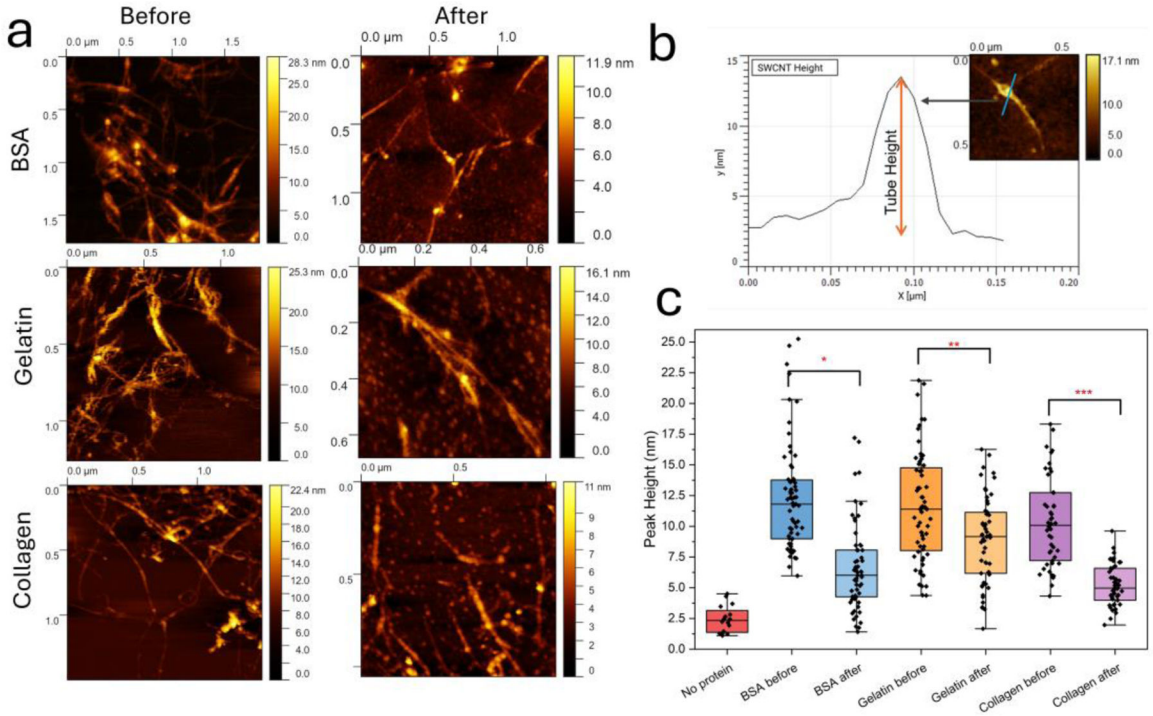

Figure 3.

AFM analysis of SWCNTs functionalized with different proteins. (a) AFM images of BSA, Gelatin, and Collagen-immobilized SWCNTs before and after enzyme reaction, showing the structural differences and degradation effect on the morphology and the aggregation of SWCNTs. (b) Height profile of a SWCNT with BSA, illustrating the tube height measurement process (inset: AFM image of the measured tube). The blue line represents the profile line drawn to extract the profile. (c) Box plot comparing the peak heights of SWCNTs functionalized with no protein, BSA, gelatin, and collagen before and after the experiment, indicating significant differences in peak heights with statistical significance marked by standard *, **, and *** (p-values 7×10^{-10}, 2×10^{-12}, 3.7×10^{-4} respectively)

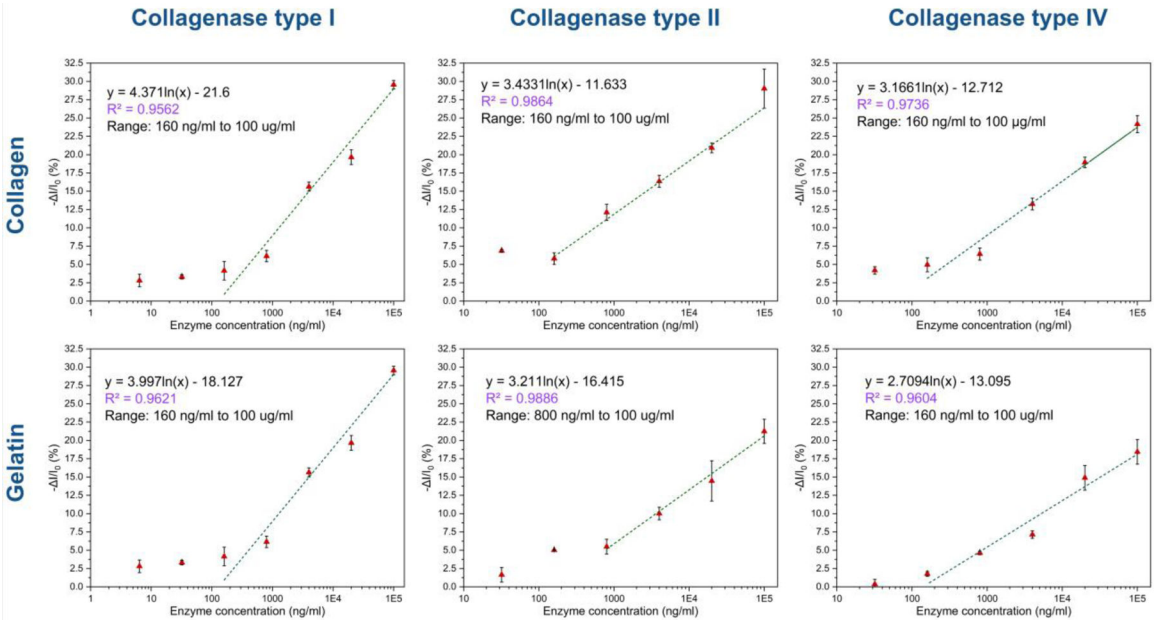

Figure 4.

Normalized signal changes of gelatin and collagen immobilized probes reacted with collagenases type I, II, and IV. The linear regression for the quantification range is plotted as a green dashed line in each plot, with the corresponding equation shown in the sub-figures. The R-squared values are also displayed as indicators of the goodness of fitting.

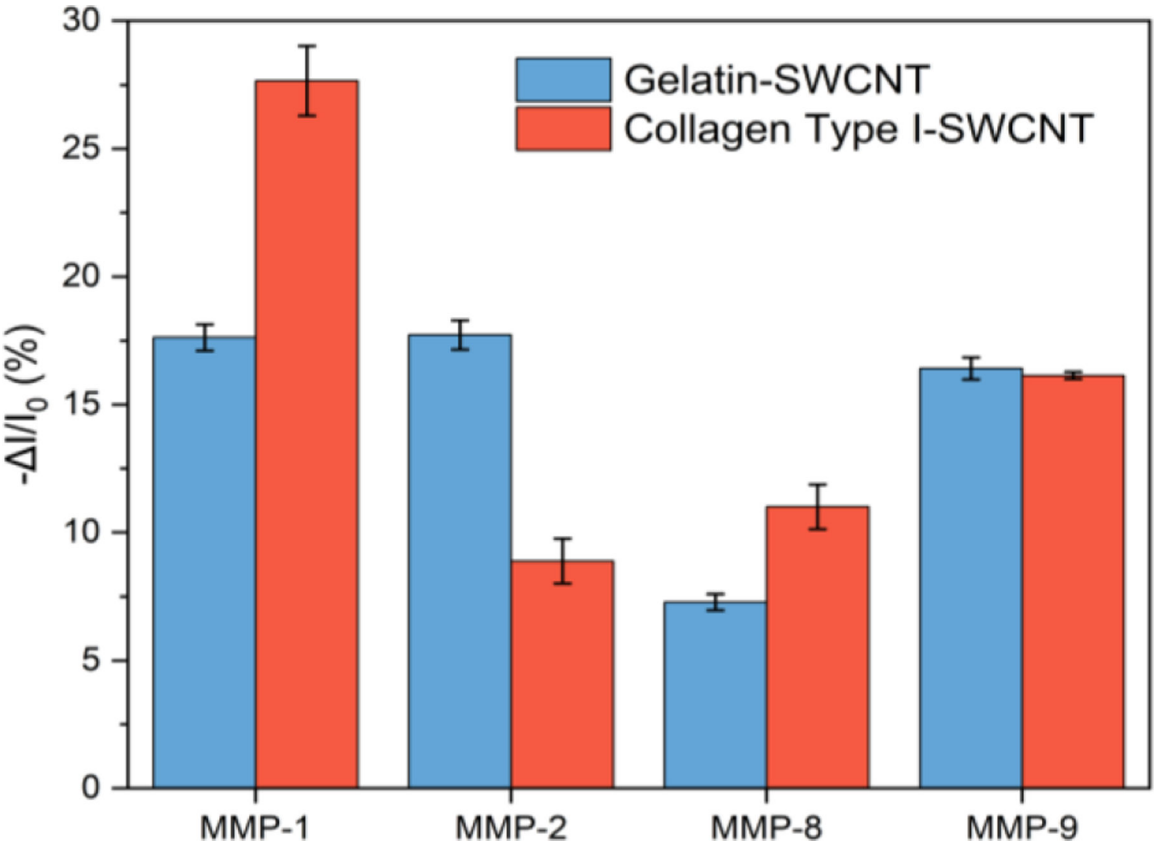

Figure 5.

Selectivity testing: comparative analysis of the percentage change in signal intensity of SWCNTs functionalized with Gelatin and Collagen Type I in response to different matrix metalloproteinases (MMP-1, MMP-2, MMP-8, and MMP-9). The data show that Collagen Type I-SWCNTs exhibit a significantly higher response to MMP-1 and MMP-8 compared to Gelatin-SWCNTs, while Gelatin-SWCNTs have a slightly higher response to MMP-9. Error bars represent the standard deviation from n=3 measurements.